

Dual Fluorescence and Excited-State Structural Relaxations in Donor–Acceptor Stilbenes

Dina Pines,[†] Ehud Pines,^{*,†} and Wolfgang Rettig^{*,‡}

Chemistry Department, Ben-Gurion University of the Negev, P. O. B. 653, Beer-Sheva 84105, Israel, and Institut für Chemie, Humboldt-Universität zu Berlin, Brook-Taylor-Str. 2, D-12489 Berlin, Germany

Received: August 17, 2001; In Final Form: July 23, 2002

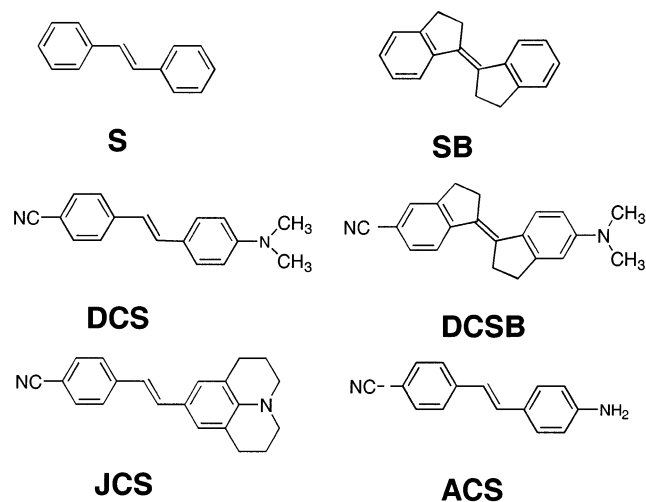
The time-resolved fluorescence behavior of two derivatives of 4-(dimethylamino)-4'-cyanostilbene (DCS) bearing a more voluminous (JCS) and less voluminous anilino group (ACS) was investigated in ethanol by reconstructing the emission spectra using picosecond time-resolved single-photon-counting technique. For JCS, these spectra exhibit a temporary isosbestic point, a clear indication of level dynamics between two emitting excited singlet states (LE and CT). Kinetic evaluation yielded a precursor–successor relationship between LE and CT and CT formation time constants of 4 ps for ACS and 8 ps for JCS. This slowing of the reaction for the compound with the larger volume of the donor moiety supports the assumption of a twisting mechanism being a major component of the reaction coordinate. An additional transient red shift of the CT band is observed for both compounds and follows the relatively slow solvation dynamics (ethanol).

1. Introduction

trans-Stilbene (S) is one of the very well studied photophysical test molecules because it exhibits an adiabatic transition to a nonemissive (dark) state, the phantom-singlet state P, which is an intermediate in the *trans*-to-*cis* isomerization process and is thought to correspond to a double-bond twisted species.^{1–4} The role of the flexibility of the adjacent single bonds has been a subject of continuing controversy. In model compounds such as “stiff stilbene” (SB), in which these bonds are rigidized, the transition to the P state can occur much faster than that for S^{5–7} and multidimensional reactive surfaces have been invoked as an explanation.^{4,8,9}

These kinetic differences between bridged and unbridged stilbene are strongly enhanced if donor–acceptor-substituted stilbene derivatives such as DCS and DCSB are investigated^{10,11} (for formulas and abbreviations, see Scheme 1). In this case, a qualitative difference was also found between the early-time behavior of these two compounds. Using picosecond fluorescence and transient absorption, Rulliere et al. have demonstrated^{10,12–14} that DCS populates a highly polar charge-transfer state, CT, after the initial excitation to the so-called locally excited state, LE, which however possesses considerable CT contributions, too.¹⁰ This transition occurs in a precursor–successor relationship thus indicating the existence of two different excited-state minima for LE and CT in polar solvents, in addition to the P state. This behavior is absent for the ring-bridged compound DCSB and suggests that the formation of the CT state is linked to the possibility of twisting the phenyl rings and that, for the description of the access to P, this additional early relaxation behavior has to be taken into account^{10,11,15–17} although previous studies could not find evidence for it.^{18–21} In view of this controversial situation challenging the existence of an additional excited state, further studies on DCS and derivatives are necessary. The multiple fluorescence of DCS was recently confirmed by several independent groups^{22,23} and extended to further derivatives.¹³

SCHEME 1: Structures of S, SB, DCS, DCSB, JCS, and ACS



Depending on the nature of the solvent, the LE to CT reaction occurs at room temperature in times ranging from 1 to 10 ps. Although these times are close to the solvent relaxation times in each case, different DCS derivatives can exhibit considerably different rates¹³ pointing to the importance of intramolecular structural changes accompanying the LE to CT transition.

In the present paper, we try to approach this question from a systematic point of view taking into account the consequences that arise from the postulation of the mechanistic model. The different behavior of DCS and DCSB suggests that this structural change is connected with a twisting of one or both phenyl groups. In this context, the theory of twisted intramolecular charge-transfer (TICT) states is helpful because it predicts the possibility for excited-state minima at twisted conformations.^{24–26} The model compounds mostly studied for the TICT process are acceptor-substituted dialkylanilines, derivatives of dimethylaminobenzonitrile (DMABN), and the adiabatic photochemical formation of the CT state is thought to involve the twisting of the dimethylamino group. The corresponding emission from the

[†] Ben-Gurion University of the Negev.[‡] Humboldt-Universität zu Berlin.

CT state is highly forbidden, in line with the small overlap of donor and acceptor orbitals.²⁴ For DCS, on the other hand, the emission from the CT state is not forbidden¹⁰ suggesting either that perpendicularity is not reached completely or that the considerably lower energy of the allowed states in the case of DCS leads to larger vibronic mixing. The TICT model can explain (i) why dual fluorescence is absent for DCSB and (ii) why it is found for DCS only in polar solvents. (i) The reactive coordinate is the twisting of one or both of the phenyl groups; (ii) although the near-planar LE state possesses considerable intramolecular charge transfer (ICT) character, the twisting of phenyl groups with their substituents leads to an electronic decoupling of the moieties and increases further the corresponding dipole moment of the CT state, which leads to a preferential energetic lowering of the twisted conformation in polar solvents.^{26,27}

In addition to comparing “stiff” model compounds such as DCSB vs DCS, a further approach to investigate the nature of the reaction coordinate leading from LE to CT consists of studying the dynamic influence of pending groups. If the twist model is correct, then the rate of twisting should be largely governed by hydrodynamic factors such as the volume of the rotating moieties and the solvent viscosity. Indeed, increasing viscosity has been confirmed to slow the transition rate from LE to CT in DCS.¹³ If, on the other hand, only solvent relaxation determined the kinetics of CT formation, different model compounds should exhibit the same rate. In this contribution, we study the influence of the size of the rotating moiety by comparing a derivative with a donor group of larger volume than in that DCS (JCS, Scheme 1) with a smaller-volume donor compound (ACS). Such a hydrodynamic approach has been previously used in the context of DMABN derivatives²⁸ and of triphenylmethane dyes^{29–31} and complements the bridging studies for “stiff” derivatives.

2. Experimental Section

Purified JCS and ACS were a gift of Karl Fischer, Bayreuth, and Helmuth Görner, Mülheim, respectively. The ethanol used was of spectroscopic quality (Merck Uvasol).

Time-resolved fluorescence spectra were obtained using the single-photon-counting setup, operated at Ben-Gurion University, described in detail elsewhere.³² The samples of $(3–5) \times 10^{-6}$ M probe molecules in ethanol solutions were excited by 1 ps pulses of a frequency-doubled Ti:sapphire laser (Tsunami, Spectra-Physics pumped by a 10 W Beamlok Ar-ion laser) operated at 82 MHz. Excitation wavelength was 348 nm using the blue optics set of the Tsunami laser. The fundamental train of pulses was pulse-selected (Spectra-Physic, model 3980) to reduce its repetition rate down to typically 0.8–4.0 MHz. The energy of the excitation pulses was 1–5 nJ/pulse. All measurements were performed under magic-angle conditions. Sample fluorescence was focused onto the entrance slit of a $1/8$ m double monochromator (CVI model 112 using a bandwidth of 2 nm) connected to a Hamamatsu 3809 6m microchannel plate photomultiplier. The full width at half-maximum (fwhm) of the instrument response function of the single-photon-counting apparatus was between 18 and 22 ps. The achievable time resolution after deconvolution was 1–2 ps in the 25 ns full-scale range of the time-to-amplitude converter (Tennelec 862). Typical counting rates were below 1 kHz. The number of counts was typically 10 K at the peak channel, collected with the Tennelec PCA3 card.

For the determination of the time-resolved fluorescence spectra, the method described by Maroncelli and Fleming was

used.^{33,34} The time- and wavelength-dependent kinetics, $D(t,\lambda)$, were measured at fixed wavelengths covering the steady-state fluorescence spectrum. The individual $D(t,\lambda)$ curves were independently fitted by a bi- or triexponential model allowing for rise and decay components using an iterative reconvolution scheme. To reconstruct the time-resolved spectra, the fitted function was scaled to the normalized steady-state spectrum, $F_{ss}(\lambda)$, according to eq 1

$$F(\lambda,t) = \frac{D(t,\lambda)F_{ss}(\lambda)}{\int_0^\infty D(t,\lambda) dt} \quad (1)$$

For wavelengths at which $F_{ss}(\lambda)$ was below 1% of its maximum value, we linked the normalization factor for a longer wavelength, at which $F_{ss}(\lambda)$ could be determined more accurately, to the ratio of the count rates observed in the respective time-resolved decays at the two wavelengths. The small variations in instrumental sensitivity over wavelengths were judged to be smaller than the errors from the direct use of the very low intensity steady-state spectrum.

To follow the temporal change in the position and form of the fluorescence spectrum, we expressed the spectrum, for each time point, in wavenumbers instead of wavelength according to $F(\nu,t) = \lambda^2 F(\lambda,t)$.

3. Results

The steady-state fluorescence spectrum of JCS in ethanol at 298 K is shown in Figure 1a, as well as the associated kinetics (Figure 1b–d) observed at three representative detection wavelengths. Applying the iterative reconvolution procedure mentioned in section 2 and using the instrument response function shown in Figure 1b, we could fit the experimental decay signal intensity $D(\lambda,t)$ in all cases to a sum of two or three exponential functions. The best fit $D(\lambda,t)$ are represented by the curves drawn in Figure 1b–d. As exemplified in Figure 1b–d, generally a fast and a slower decaying component were observed in the blue wing of the spectrum, while distinctive rise times were found in the red part of the spectrum. At intermediate wavelengths (Figure 1c), more complicated decays were observed indicating the presence of two emitting species.

The set of fitted transients provided reconstructed transient fluorescence spectra consisting of 15 frequency points at any given time in the time interval from 3 ps to 6 ns. Figure 2 presents the time-resolved reconstructed emission spectra obtained during the first 80 ps after the excitation. A clearly visible temporal isoemissive point at $18\,520\text{ cm}^{-1}$ (540 nm) indicates the presence of two excited states linked by a precursor–successor relationship, assigned to a short-lived LE state and a more red-shifted longer-lived CT state.

These spectra were fitted to the sum of two Gaussian line-shape functions (eq 2) providing an acceptable fit of the data in all cases. Alternative fits to the sum of two log-normal functions were also possible but somewhat less satisfactory and were not used.

$$F(\nu,t) = I \exp\left(-\frac{(\nu - \nu_p)^2}{2w^2}\right) \quad (2)$$

Three parameters, the integrated fluorescence intensity I , the width parameter w , where the full width at half-maximum is $\Gamma = 2w\sqrt{\ln 4}$, and the peak frequency ν_p , for each excited state are determined in a nonlinear least-squares fitting procedure for each transient spectrum. To the extent that a Gaussian function

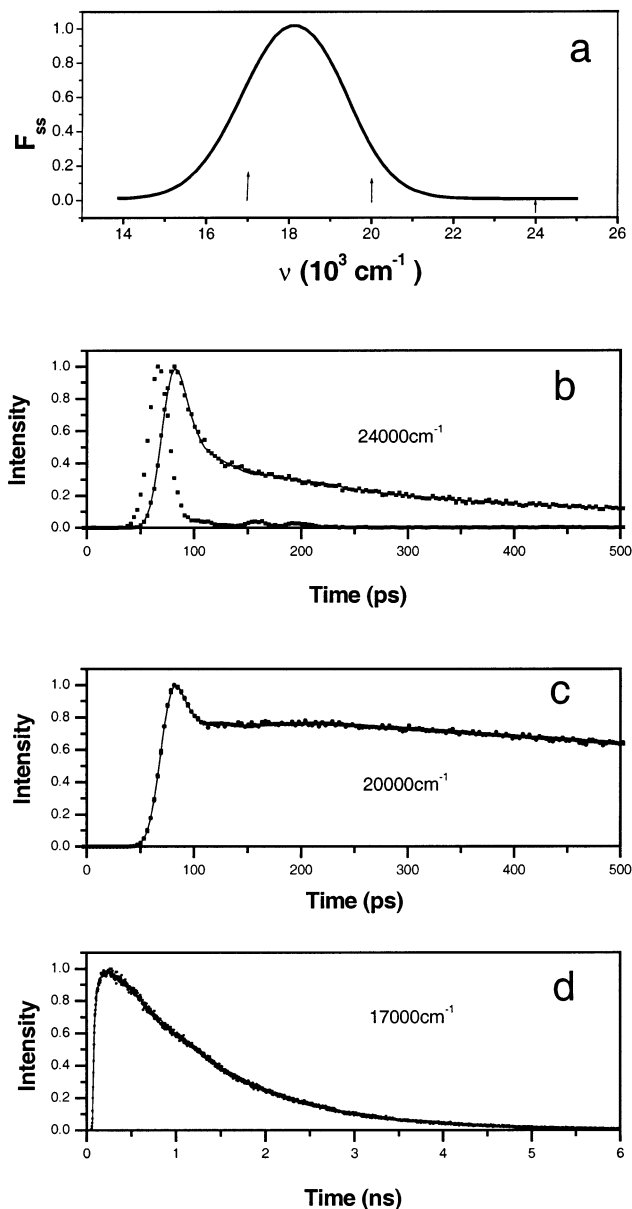


Figure 1. (a) Steady-state fluorescence spectrum of JCS in ethanol at 298 K and (b–d) fluorescence decay traces at three representative emission wavelengths indicated by arrows in panel a. Panel b also contains the instrument function of the setup used.

accurately represents $F(\nu, t)$, the evolution of these parameters in time determines the observed dynamics of the two states.

The decomposition of the fluorescence of JCS in ethanol into two subbands at four representative time points is shown in the Supporting Information and can be summarized as follows. The fluorescence spectra in ethanol show the development of a red-shifted band at $18\,230\text{ cm}^{-1}$ (549 nm) from what has been a shoulder in the spectrum recorded immediately after excitation and a corresponding fall of the short-wavelength band at $19\,230\text{ cm}^{-1}$ (520 nm). At longer times, the lower-energy CT band grows in relative importance.

The decay of the integrated fluorescence of the LE band and the corresponding growth of the CT band for JCS are shown in Figure 3. The integral of the total time-resolved fluorescence spectrum (CT + LE) is nearly time-independent. The formation of the CT band is delayed with respect to the excitation pulse with a clear rise time as shown in Figure 3a. The rise time of the CT state is found to be $8 \pm 2\text{ ps}$, matching the decay time

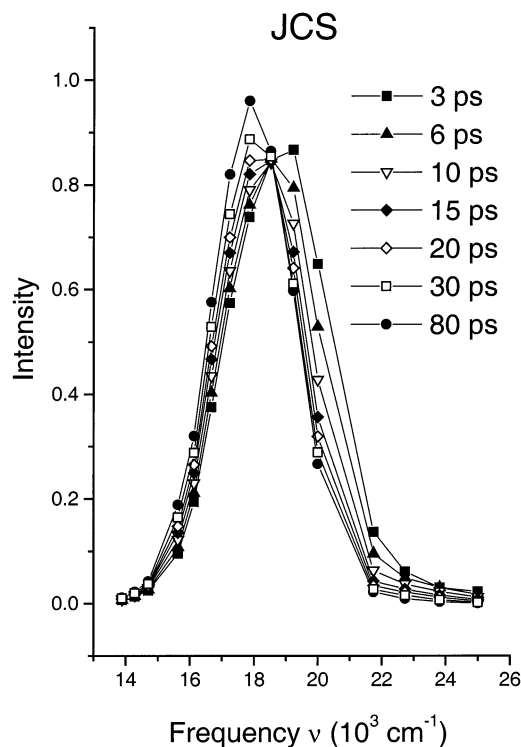


Figure 2. Time-resolved emission spectra of JCS in ethanol at 298 K reconstructed from emission decay curves. An isoemissive point is observed at 540 nm ($18\,520\text{ cm}^{-1}$).

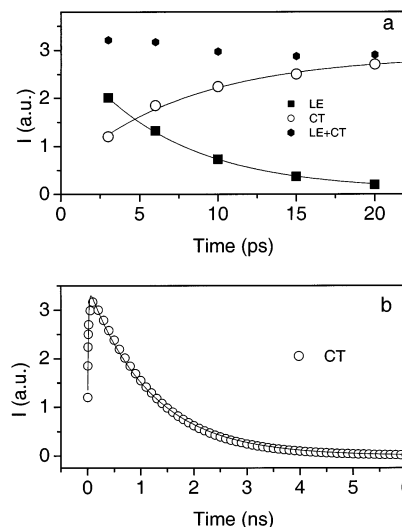


Figure 3. Decay of the LE and growth of the CT band for JCS in ethanol at 298 K. The integral of the total time-resolved fluorescence spectrum (CT + LE) is nearly time-independent. On a longer time scale, the fast rise (8 ps) and much slower decay (1.15 ns) of the CT band can be observed (lower part of figure).

of the LE state. On a longer time scale, the much slower decay ($1.15 \pm 0.05\text{ ns}$) of the CT band is observed (Figure 3b). The evolution of the dynamic Stokes shift of the low-energy state of JCS in ethanol from 549 to 558 nm is shown in Figure 4.

Figure 5 presents the reconstructed emission spectra obtained for ACS in ethanol during the first 200 ps after the excitation. (A figure with the dual fluorescence behavior of ACS at four representative time points can be found in the Supporting Information). The fluorescence spectra in ethanol show the fast development of a red-shifted band at $20\,200\text{ cm}^{-1}$ (495 nm) and a corresponding decrease of the short-wavelength band at

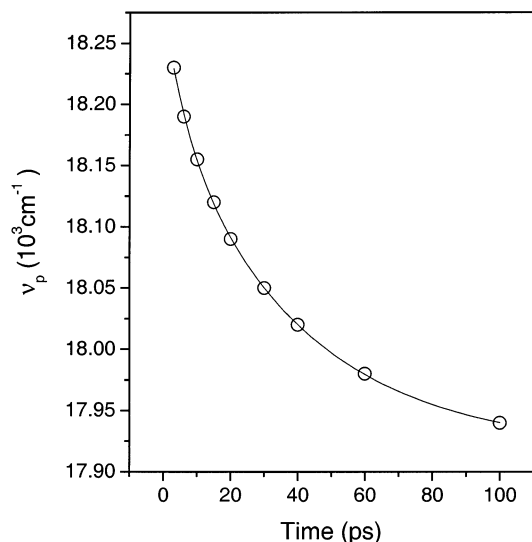


Figure 4. Red shift of the CT band of JCS in ethanol as a function of time. The solid curve corresponds to a biexponential decay with $\tau_1 = 7$ ps (23%) and $\tau_2 = 38$ ps (76%).

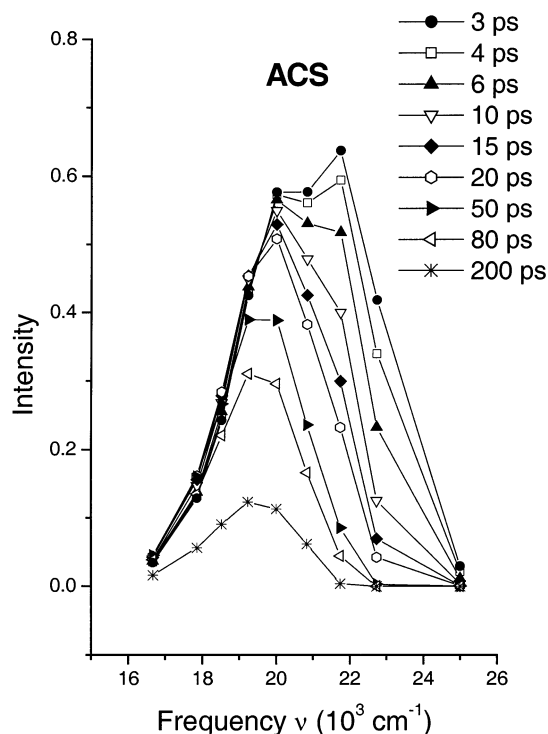


Figure 5. Reconstructed time-resolved emission spectra of ACS in ethanol at 298 K.

21 980 cm^{-1} (455 nm). The decay of the integrated fluorescence of the LE band and the growth of the CT band for ACS in ethanol are shown in Figure 6. The formation of the CT band is delayed with respect to the excitation pulse with a clear rise time as shown in Figure 6a. The rise time of CT state is found to be 4 ± 1 ps matching the decay time of the LE band. On a longer time scale, the slower decay (110 ± 5 ps) of the CT band is observed (Figure 6b). The fluorescence lifetime of the CT state of ACS is short as compared to the fluorescence lifetime of JCS (1.15 ns). The evolution of the dynamic Stokes shift of the low-energy state of ACS in ethanol from 495 to 515 nm is shown in Figure 7.

The time evolution of the dynamic Stokes shift of the CT state of JCS (Figure 4) was fitted by the sum of two exponentials

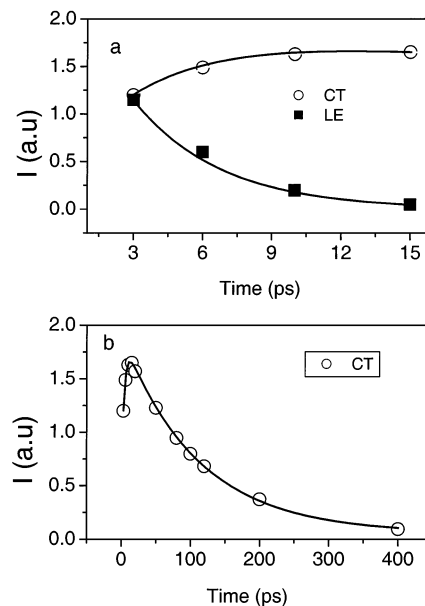


Figure 6. Decay of the LE and growth of the CT band for ACS in ethanol at 298 K. On a longer time scale, the fast rise (4 ps) and slower decay (110 ps) of the CT band can be observed (lower part of the figure).

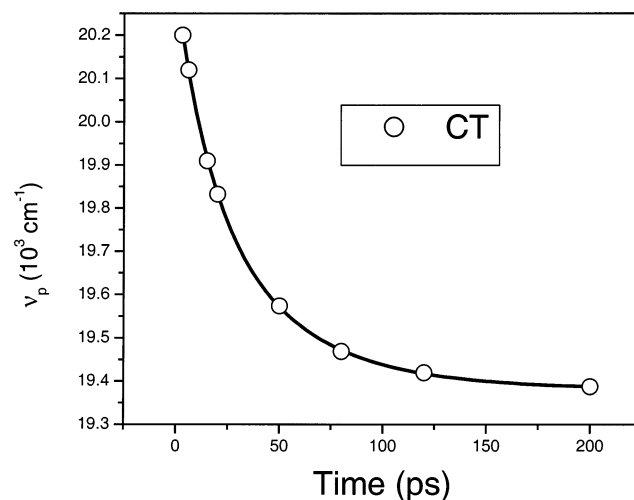


Figure 7. Red shift of the CT band of ACS in ethanol as a function of time. The solid curve corresponds to a biexponential decay with $\tau_1 = 6$ ps (20%) and $\tau_2 = 36$ ps (80%).

with time constants $\tau_1 = 7 \pm 1$ ps (23%) and $\tau_2 = 38 \pm 3$ ps (76%). The weighted average time constant is about 30 ps. The time evolution of the dynamic Stokes shift of the CT state of ACS (Figure 7) has two very similar time constants $\tau_1 = 6 \pm 1$ ps (20%) and $\tau_2 = 36 \pm 3$ ps (80%) and the same weighted average time constant of about 30 ps. This average time constant is similar to the longitudinal relaxation time of the solvent.³⁵ The observed relaxation times compare well with previously determined multiexponential dynamic Stokes shifts in ethanol.³⁶

4. Discussion

4.1. Dual Fluorescence. From the results of the CT rise times observed here (4 ps for ACS, 8 ps for JCS), we can anticipate similarly fast time constants for DCS. Indeed, time-resolved studies on DCS have established a similar dual fluorescence and comparable time constants.^{13,22,23}

The dual fluorescence of DCS therefore occurs on a time scale that is very short compared to the excited-state lifetime

such that the integrated or steady-state emission consists of virtually pure emission from the CT state formed by the excited-state process. Moreover, the spectra of the primary state LE and those of CT are not shifted much relative to each other, so the steady-state spectra of different DCS model compounds with and without a channel to the CT state differ only very little.¹⁰ This is the reason that fast and precise time-resolved methods have to be used to detect the dual fluorescence. For the same reason, we chose ethanol and not the faster-relaxing acetonitrile because we hoped to separate between the solvation process and the TICT dynamics.

In an early attempt, very strong picosecond pulses from amplified lasers and very high concentrations were used, and a transition between two fluorescence bands significantly differing in position was reported.³⁷ These species were later recognized as being due to complexation between two excited DCS species (bimer) because they disappear upon dilution and reduction of excitation intensity,³⁸ and only recently it has been substantiated that a precursor–successor relationship can nevertheless be observed in dilute solutions and at low excitation intensities that can be ascribed to a monophotonic monomolecular process.^{22,13} In view of these complications, it is therefore of importance that in the present study, a single-photon-counting experiment using low excitation intensity and micromolar solutions confirms these results consistently. The fact that the precursor–successor behavior is not observed for DCS in nonpolar solvents nor for the bridged compound DCSB in both polar and nonpolar solvents can be taken as evidence that a single bond twisting process around one of the ethylene–phenyl bonds leading to a more polar CT state is taking place.¹³ The presence of the dual fluorescence as revealed here also for JCS in which the dialkylamino group is blocked confirms this conclusion and supports earlier studies stating that the twisting of the smaller dialkylamino group is not important for the reaction coordinate.³⁹ The interpretation of a twisting anilino group for CT formation in DCS is further supported by the observation of dual fluorescence also for the amino-substituted compound ACS. In contrast to the behavior of DMABN, we can therefore conclude that the twisting moiety is not the amino or dialkylamino group but the anilino or dialkylanilino moiety. This conclusion was reached previously¹⁵ and is supported by recent *ab initio* calculations.^{40,41} Although in previous studies^{10–17} the behavior of bridged compounds indirectly suggested the involvement of a twisting process, in this study, the twisting is more directly demonstrated by the viscosity and rotator size effect, and dual fluorescence is observed even in the case of ACS.

It may seem astonishing that an anilino group twists in the excited state, given that bond order considerations predict this single bond to be strengthened, as in stilbene itself, and even more through the donor–acceptor interactions, which introduce quinoid character into the wave function. However, this reasoning does not hold for perpendicular conformations, and their energetics are dictated by the donor–acceptor properties of the moieties, as given by the theory of biradicaloid charge-transfer states.^{26,42,43} If these twisted conformations are energetically low-lying, they will be accessible photochemically, possibly by overcoming a more or less small activation energy. This activation energy can be considerably reduced by the involvement of conical intersections between excited states.^{25,44}

4.2. Influence of the Rotational Volume. The observed kinetics for the LE to CT transition in DCS are in the range around and below 10 ps and depend on viscosity. For DCS, values of 4 ps in methanol and 10 ps in butanol have been

TABLE 1: Observed Relaxation Times for the CT Emission in Ethanol at 298 K

	τ_{rise}	τ_{decay}	τ_{shift}
JCS	8 ± 2 ps ^a	1.15 ± 0.05 ns	7 ± 1 ps (23%) 38 ± 3 ps (76%)
ACS	4 ± 1 ps ^a	110 ± 5 ps	6 ± 1 ps (20%) 36 ± 3 ps (80%)
DCS	$5\text{--}7$ ps ^b	300 ± 15 ps ^c	

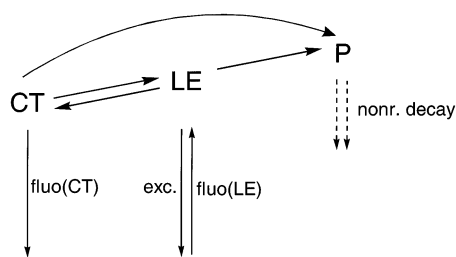
^a Evaluated from spectral and band integration (see Figures 3 and 6) for both LE and CT emissions. ^b Linear interpolation from the data in ref 13. ^c Evaluated from several decay traces at different wavelengths.

reported,¹³ and with a linear viscosity interpolation, around 5–7 ps is expected for ethanol. In the twisting model, these rates, if compared in one given solvent, should depend on the size of the rotating moiety. Experimentally, the change from ACS to DCS to JCS leads to a significant slowing of the reaction by a factor of around 2 (Table 1). This observation supports the use of the twisting mechanism from a dynamic point of view and establishes the importance of large-amplitude (twisting) motions of the anilino group for the CT reaction to occur.

It could be argued, as is usually the case when electron transfer is involved, that factors other than large amplitude motions such as free energy changes, ΔG , induced by the variation of the donor groups mainly control the observed rate constants. In this case, one would expect that the donor character will influence the energy of both LE and CT states because they both possess significant CT character.¹⁰ But the CT state, being more strongly polar,¹³ will be influenced more strongly. The donor character increases in the series aniline, dimethylaniline, julolidine, and therefore, JCS is expected to possess a stronger energetic lowering and correspondingly exergonic (negative) ΔG than ACS. In a Marcus-type forward electron-transfer reaction in the normal region, this should lead to increased rate constants for JCS as compared to ACS in a given solvent, contrary to observation. The increased hydrodynamic friction for JCS therefore reduces the value for JCS below that of ACS.

However, the reported relatively small difference (factor 2.5) between the transition rate of DCS in methanol and butanol where both solvent polarity and hydrodynamic factors are expected to slow the rate implies that a simple Marcus-type mechanism is probably not the important factor in this case, either because it is not the controlling mechanism or because the reaction is in a region where it is weakly sensitive to changes in ΔG . The latter case arises for nearly activationless processes or at the inflection point between the normal and the inverted region. In such cases, the reaction rate is controlled by the preexponential factor, which is usually determined by the solvent relaxation dynamics. In our case, the observed transition rates for ACS and JCS (4 and 8 ps, respectively) are faster than τ_L , the longitudinal dielectric relaxation time of the solvent (30 ps, the average relaxation time of ethanol), and are clearly shown to be also solute-dependent (JCS vs ACS) pointing to the importance of an intramolecular relaxation (see below). Both observations favor an adiabatic transfer mechanism over a Marcus-type weak interaction model.

Very similar results were found for a related series of molecules belonging to the family of triphenylmethane (TPM) dyes.^{29–31,45} In this case, too, the anilino derivative was the fastest to react toward a nonemitting charge-localized state also connected with electron transfer and twisting of anilino groups, and the rate factor between the dimethylanilino and the julolidino compound was around 1.3–1.8, consistent with the present results and with the increase of the rotational volume for these

SCHEME 2: Three-State Mechanistic Model^a

^a The initial relaxation is downhill to CT. From CT, the endothermic P state may be reached indirectly via LE or directly. This corresponds to a different reaction path within the two-dimensional hypersurface defined by single- and double-bond twisting.

two types of rotors.³⁰ TPM dyes are generally believed to possess barrierless reaction profiles, which can be modeled by driven diffusion.^{46,47} In the case of DCS and derivatives, the reaction rates observed are nearly as fast as those for the TPM dyes. This is a possible indication that in this case, too, a barrierless reaction is involved.

A further possibility to interpret the observed rate constants is the relaxation of a dipolar LE state without involvement of a more polar CT state. In this case, time-dependent shifts of a single band would be expected. The fast (4–8 ps) component could be due to vibrational relaxation, the longer one (see below) to solvation. This model, however, does not explain why ACS has the fastest short-time kinetics and JCS the slowest one nor why temporary isosbestic points and dual fluorescence band shapes are observed (Figures 2 and 6).

4.3. Electron Transfer and Solvent Relaxation Times.

Electron-transfer reactions are often controlled by solvent relaxation.⁴⁸ In such cases, the reaction rate is inversely proportional to the dielectric relaxation time of the solvent. The widely differing reaction rates for ACS, DCS, and JCS in the same solvent indicate that the reaction is not simply controlled by solvent relaxation but that intramolecular motion is also important. This is especially consistent with an energetically barrierless or even downhill nature of the reactive hypersurface where the reaction is controlled by diffusional kinetics.⁴⁷ In principle, nonexponential time dependences are expected for

pure barrierless reactions,⁴⁷ but with the present time resolution, such a behavior cannot be discriminated from an exponential behavior.

When solvation is the only decisive factor for a given relaxation process, then dynamics of any given compounds such as JCS and ACS are equal. This is indeed the case for the kinetics of the red shift of the CT band (main component ca. 36 ps, Table 1), which is similar to that observed for other fluorescent molecules.³⁶

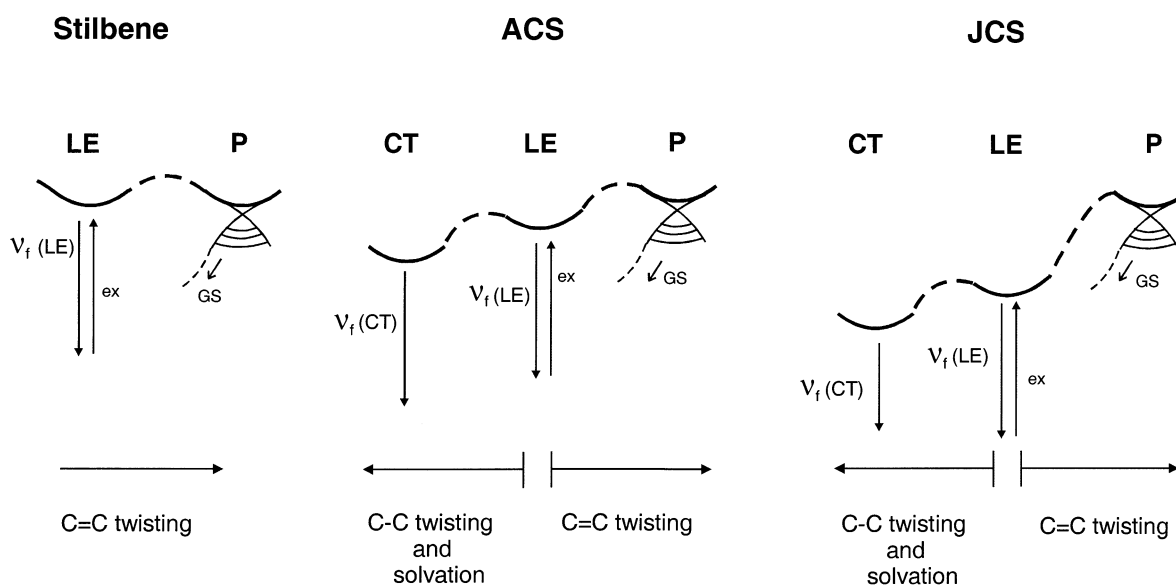
4.4. The Endothermic Access to the Conical Intersection

(Phantom Singlet State P). The three DCS derivatives possess strikingly different decay constants of the CT state: just 110 ps for ACS, 300 ps for DCS, and 1.15 ns for JCS. The very long lifetime of JCS is consistent with the results of a previous study of this compound in which anomalously high fluorescence quantum yields were observed.⁴⁹

To explain this contrasting behavior, Scheme 2 can be used, taking into account the dipolar properties of the states involved: LE and CT are both highly polar with an increased dipole moment for CT, but P has nonpolar or weakly polar properties^{11,26} and is therefore considerably less stabilized when the solvent polarity increases. Increasing solvent polarity therefore stabilizes both LE and CT but much less P. This is the reason why the nonradiative decay rate, which is governed by the access to P (double-bond twisting), decreases with an increase of solvent polarity.^{11,18,26}

The energy of these states is likewise influenced by the quality of the donor: For increased donor properties (julolidino group), both states with CT character will be significantly lowered but the energy of the P state will largely remain unaffected. Given the fact that LE and P states are roughly isoenergetic in *trans*-stilbene,⁵⁰ it can even be envisaged that the access to P is slightly endothermic in DCS derivatives because of the additional stabilization by populating the CT state. The endothermicity will then be largest for JCS with the best donor group and the strongest stabilization of CT and will be smallest for ACS. This much better thermal availability of an endothermic P state for ACS explains its much shorter fluorescence lifetime.

Endothermic access to the P state is consistent with efficient nonradiative decay, if the coupling to the ground state is very

SCHEME 3: Schematic Representation of Excited-State Reactive Surface^a

^a After excitation to LE, donor–acceptor stilbenes have an additional relaxation channel that leads to CT and shows up in dual fluorescence; the P state is endothermic, most strongly for JCS.

strong. A strong coupling is not possible if the energy gap between P and the ground state is large. Indeed, the best model for an efficient coupling between P and S_0 in stilbene seems to be a conical intersection.^{51,52} This situation is schematically shown in Scheme 3 for the three compounds stilbene, ACS, and JCS.

Usually, double-bond-twisting reactions in smaller molecules evolving through conical intersections occur in the femtosecond time range⁵³ and do not necessitate several hundred picoseconds as observed here. This time scale points to an activated process. The P state in the DCS derivatives therefore seems to be a region in phase space with double-bond twisted geometry and femtosecond access to the nearly isoenergetic ground state, but this region is energetically higher lying and has to be reached thermally, and this controls and slows the observed rate.

5. Conclusions

The results reported for two different donor–acceptor stilbene derivatives provide evidence of dual emission in the picosecond time range and support the view that not only double-bond twisting but also single-bond twisting processes are important for this type of molecules. The substituent and bridging pattern tested strongly support the involvement of the single-bond twist around the anilino–ethylene bond to be part of the reaction coordinate. The strongly different fluorescence lifetimes observed can be explained with a model involving an activated access to a conical intersection linking ground and excited state (the so-called phantom singlet state P).

Note Added in Proof. Quite recently a fluorescence upconversion study of DCS appeared (Kovalenko, S. A.; Schanz, R.; Senyushkina, T. A.; Ernsting, N. P. *Phys. Chem. Chem. Phys.* **2002**, *4*, 703) where it was concluded that the dual fluorescence observed previously for DCS was an artifact due to reabsorption by the highly populated S_1 state. The dual fluorescence dynamics observed are explained to be indirectly due to the time-dependent red shift of the fluorescence band. Our study brings new arguments in this connection: Dual fluorescence is also observed for our low-concentration low-excitation-intensity conditions with weak S_1 population, and the dynamics is different for different compounds, unlike as would be expected from the above explanation. The systems investigated in the two studies differ, however, in a very important point: The present study uses ethanol as solvent which is a “slow” solvent, i.e., solvation dynamics is slower than the reaction observed. In the study of Kovalenko et al., acetonitrile was used as solvent which is “fast”, i.e., the reaction is expected to occur for solvent equilibrated conditions. The problem is not solved yet and deserves further studies.

Acknowledgment. We thank Dr. Karl Fischer and Dr. Helmut Görner, Mülheim, for gifts of the samples of JCS and ACS, respectively.

Supporting Information Available: Figure showing the dual fluorescence behavior of ACS at four representative points. This material is available free of charge via the Internet at <http://pubs.acs.org>.

References and Notes

- (1) Saltiel, J.; D'Agostino, J.; Megarity, E. D.; Metts, L.; Neuberger, K. R.; Wrighton, M.; Zafriou, O. C. In *Organic Photochemistry*; Chapman, O. L., Ed.; Marcel Dekker: New York, 1973; Vol. 3, Chapter 1, p 1.
- (2) Saltiel, J.; Charlton, J. L. In *Rearrangements in Ground and Excited States*; de Mayo, P., Ed.; Academic Press: New York, 1980; Vol III, p 25.
- (3) Saltiel, J.; Sun, Y.-P. In *Photochromism, Molecules and Systems*; Dürr, H., Bouas-Laurent, H., Eds.; Elsevier: Amsterdam, 1990; p 64.
- (4) Waldeck, D. *Chem. Rev.* **1991**, *91*, 415.
- (5) Saltiel, J.; D'Agostino, J. T. *J. Am. Chem. Soc.* **1972**, *94*, 6445.
- (6) Rothenberger, R.; Negus, D. K.; Hochstrasser, R. M. *J. Chem. Phys.* **1983**, *79*, 5360.
- (7) Schneider, S.; Brem, B.; Jäger, W.; Rehabe, H.; Lenoir, D.; Frank, R. *Chem. Phys. Lett.* **1999**, *308*, 211.
- (8) Park, N. S.; Waldeck, D. H. *J. Chem. Phys.* **1989**, *91*, 943.
- (9) Agmon, N.; Kosloff, R. *J. Phys. Chem.* **1987**, *91*, 1988.
- (10) Lapouyade, R.; Czeschka, K.; Majenz, W.; Rettig, W.; Gilabert, E.; Rullière, C. *J. Phys. Chem.* **1992**, *96*, 9643.
- (11) Rettig, W.; Majenz, W.; Herter, R.; Létard, J. F.; Lapouyade, R. *Pure Appl. Chem.* **1993**, *65*, 1699.
- (12) Viallet, J.-M.; Dupuy, F.; Lapouyade, R.; Rullière, C. *Chem. Phys. Lett.* **1994**, *222*, 571.
- (13) Abraham, E.; Oberle, J.; Jonusauskas, G.; Lapouyade, R.; Rullière, C. *Chem. Phys.* **1997**, *214*, 409.
- (14) Abraham, E.; Oberle, J.; Jonusauskas, G.; Lapouyade, R.; Rullière, C. *J. Photochem. Photobiol., A: Chem.* **1997**, *105*, 101.
- (15) Letard, J.-F.; Lapouyade, R.; Rettig, W. *Chem. Phys.* **1994**, *186*, 119.
- (16) Rettig, W.; Majenz, W.; Lapouyade, R.; Haucke, G. *J. Photochem. Photobiol., A: Chem.* **1992**, *62*, 415.
- (17) Létard, J. F.; Lapouyade, R.; Rettig, W. *J. Am. Chem. Soc.* **1993**, *115*, 2441.
- (18) Rettig, W.; Majenz, J. *Chem. Phys. Lett.* **1989**, *154*, 335.
- (19) Il'ichev, Y. V.; Kühnle, W.; Zachariasse, K. A. *Chem. Phys.* **1996**, *211*, 441.
- (20) Gruen, H.; Görner, H. *Z. Naturforsch.* **1983**, *38A*, 928.
- (21) Safarzadeh-Amiri, A.; *Chem. Phys. Lett.* **1986**, *125*, 272.
- (22) Eilers-König, N.; Kühne, T.; Schwarzer, D.; Vöhringer, P.; Schroeder, J. *Chem. Phys. Lett.* **1996**, *253*, 69.
- (23) Papper, V.; Likhtenshtein, G.; Pines, D.; Pines, E. *Rec. Res. Devel. Photochem., Photobiol.* **1998**, *1*, 205 (Transworld Research Network, Trivandrum, India).
- (24) Grabowski, Z. R.; Rotkiewicz, K.; Siemiarczuk, A.; Cowley, D. J.; Baumann, W. *Nouv. J. Chim.* **1979**, *3*, 443.
- (25) Rettig, W. *Angew. Chem., Int. Ed. Engl.* **1986**, *25*, 971.
- (26) Rettig, W. In *Topics in Current Chemistry, Electron-Transfer I*; Mattay, J., Ed.; Springer-Verlag: Berlin, 1994; Vol. 169, p 253.
- (27) Maus, M.; Rettig, W.; Bonafoux, D.; Lapouyade, R. *J. Phys. Chem. A* **1999**, *103*, 3388.
- (28) Rettig, W. *J. Phys. Chem.* **1982**, *86*, 1970.
- (29) Vogel, M.; Rettig, W. *Ber. Bunsen-Ges. Phys. Chem.* **1985**, *89*, 962.
- (30) Rettig, W.; Vogel, M. *Ber. Bunsen-Ges. Phys. Chem.* **1987**, *91*, 1241.
- (31) Rettig, W. *Appl. Phys.* **1988**, *B45*, 145.
- (32) Pines, E.; Pines, D.; Barak, T.; Magnes, B.-Z.; Tolbert, L. M.; Haubrich, J. E. *Ber. Bunsen-Ges. Phys. Chem.* **1998**, *102*, 511.
- (33) Maroncelli, M.; Fleming, G. R. *J. Chem. Phys.* **1987**, *86*, 6221.
- (34) Castner, E. W., Jr.; Maroncelli, M.; Fleming, G. R. *J. Chem. Phys.* **1987**, *86*, 1090.
- (35) Barthel, J.; Buchner, R. *Pure Appl. Chem.* **1991**, *63*, 1473.
- (36) Horng, M. L.; Gardecki, J. A.; Papazyan, A.; Maroncelli, M. *J. Phys. Chem.* **1995**, *99*, 17311.
- (37) Gilabert, E.; Lapouyade, R.; Rullière, C. *Chem. Phys. Lett.* **1988**, *145*, 262.
- (38) Gilabert, E.; Lapouyade, R.; Rullière, C. *Chem. Phys. Lett.* **1991**, *185*, 82.
- (39) Gruen, H.; Görner, H. *J. Phys. Chem.* **1989**, *93*, 7144.
- (40) Amatatsu, Y. *Theor. Chem. Acc.* **2000**, *103*, 445.
- (41) Amatatsu, Y. *Chem. Phys.* **2001**, *274*, 87.
- (42) Michl, J.; Bonacic-Koutecký, V. *Electronic Aspects of Organic Photochemistry*; J. Wiley & Sons: New York, 1990.
- (43) Grabowski, Z. R.; Rotkiewicz, K.; Rettig, W.; Structural changes accompanying intramolecular electron transfer – focus on T. I. C. T. states and structures. *Chem. Rev.*, submitted for publication, June 2001.
- (44) Zilberg, S.; Haas, Y. *J. Phys. Chem. A* **2002**, *106*, 1.
- (45) Jurczok, M.; Plaza, P.; Martin, M. M.; Rettig, W. *J. Phys. Chem. A* **1999**, *103*, 3372.
- (46) Förster, T.; Hoffmann, G. *Z. Phys. Chem. Neue Folge* **1971**, *75*, 63.
- (47) Bagchi, B.; Fleming, G. R.; Oxtoby, D. W. *J. Chem. Phys.* **1983**, *78*, 7375.
- (48) Kosower, E. M.; Huppert, D. *Annu. Rev. Phys. Chem.* **1986**, *37*, 127.
- (49) Reithaler, K.; Köhler, G. *Chem. Phys. Lett.* **1996**, *250*, 152.
- (50) Saltiel, J.; Waller, A. S.; Sears, D. F., Jr. *J. Am. Chem. Soc.* **1993**, *115*, 245.
- (51) Bernardi, F.; Olivucci, M.; Robb, M. A. *J. Photochem. Photobiol., A: Chem.* **1997**, *105*, 365.
- (52) Amatatsu, Y. *Chem. Phys. Lett.* **1999**, *314*, 364.
- (53) Fuss, W.; Lochbrunner, S.; Müller, A. M.; Schikarski, T.; Schmid, W. E.; Trushin, S. A. *Chem. Phys.* **1998**, *232*, 161.